Direct-Ink Write 3D Printing Multi-Stimuli-Responsive Hydrogels and Post-Functionalization Via Disulfide Exchange

Christopher R. Fellin and Alshakim Nelson[*a]

[a]Department of Chemistry, University of Washington, Seattle, Washington 98105, USA

KEYWORDS: Hydrogel, Stimuli-Responsive, Polymer Network, Post-functionalization, Pyridyl Disulfide, Temperature Response, 3D Printing

ABSTRACT Herein, we describe a multi-stimuli-responsive hydrogel that can be 3D printed via a direct-ink write process to afford cross-linked hydrogel networks that can be post-functionalized with thiol-bearing molecules. Poly(alkyl glycidyl ether)s with methacrylate groups at their termini were synthesized and self-assembled into hydrogels with three key stimuli-responsive behaviors necessary for extrusion based 3D printing: a sol-gel temperature response, shear-thinning behavior, and the ability to be photochemically crosslinked. In addition, the chemically crosslinked hydrogels demonstrated a temperature dependent swelling consistent with an LCST behavior. Pyridyl disulfide urethane methacrylate (PDS-UM) monomers were introduced

into the network as a thiol-reactive handle for post-functionalization of the hydrogel. The reactivities of these hydrogels were investigated at different temperatures (5, 25, 37 °C) and swelling statuses (as-cured versus preswollen) using glutathione as a reactive probe. To illustrate the versatility of the platform, a number of additional thiol-containing probes such as proteins, polymers, and small molecules were conjugated to the hydrogel network at different temperatures, pH's, and concentrations. In a final demonstration of the multi-stimuli-responsive hydrogel platform, a customized DIW 3D printer was used to fabricate a printed object that was subsequently conjugated with a fluorescent tag and displayed the ability to change in size with environmental temperature.

1. INTRODUCTION

Hydrogels are water-swollen networks of macromolecules bound by chemical or physical crosslinks. Their soft nature and inherently high water content (typically 70-99%) mimic the natural environment of living tissues, making them ideal for tissue engineering[1–3] and wound healing applications.[4,5] Stimuli-responsive hydrogels react to environmental cues such as temperature,[6] light,[7] or mechanical stress[8,9] to induce a chemical or physical change in material properties. These hydrogels have recently been adopted in the field of additive manufacturing (also referred to as 3D printing), a technique that utilizes computer aided hardware and software for the sequential deposition of a material to fabricate three-dimensional objects.[10,11] Direct-ink write (DIW) 3D printing is one such method that can use shear-thinning hydrogels to facilitate the flow of material through fine resolution nozzles.[12–15] Shear-thinning responses enable effective printing

while other stimuli-responses can introduce added functionality after printing such as actuation,[16–18] shape memory,[19–21] and pH dependent drug release.[22,23]

Stimuli-responsive triblock copolymers can afford versatile gel-based inks for DIW 3D printing.[24–29] Our group has investigated and developed poly(alkyl glycidyl ether)-based hydrogels that exhibit temperature-, shear-, and light-responsive properties.[30–32] The sol-gel temperature response enables facile homogenization of additives while the shear-thinning response facilitates the extrusion of the material from the printhead nozzle and generates the 3D printed object. The material can then be chemically cross-linked using photo-initiated free radical polymerization to create robust objects capable of withstanding dissolution and deformation.

The conjugation of molecules to hydrogel materials under mild conditions with high specificity offers a straightforward method to functionalize these systems.[33–38] For instance, the Anseth group developed a PEG/protein hydrogel with orthogonal alkene functionality for the conjugation of photopatterned biomolecules. Thiol-ene click chemistry was used to modify the existing hydrogel with the cell-adhesion tripeptide motif Arg-Gly-Asp (RGD) for cell attachment with spatial control.[39] Alternatively, azide-alkyne click reactions were utilized by Sanyal and coworkers for the post-functionalization of dendron-polymer conjugate hydrogels. While some of the alkynes were utilized as crosslinking points to form the hydrogel, residual alkyne groups were available for the covalent attachment of additional azide-containing molecules including fluorescent dyes (4-azido-N-ethyl-1,8-naphthalimide and BODIPY) and biotin for protein immobilization.[40] Adapting such techniques to the post-functionalization of 3D printed systems could enable facile modification of hydrogel materials for a multitude of post-print applications.

Pyridyl disulfide is a versatile motif used in a number of applications to conjugate thiol-bearing molecules.[41] The efficient thiol-pyridyl disulfide exchange enables conjugation of small-to-large

molecule reactants including peptides,[42–44] proteins,[45–47] and even RNA[48–50] with high specificity under mild conditions. Additionally, the 2-pyridothione leaving group has a convenient absorbance spectrum that allows for methodical tracking of conjugation rates by monitoring the evolution of the 343 nm absorbance peak via UV-Vis spectroscopy.

While the utilization of pyridyl disulfides in polymeric systems has been investigated, its use as a reactive functionality towards the post-functionalization of hydrogels has not been thoroughly explored. One recent example includes work by Sanyal and co-workers to post-functionalize PEG hydrogels with thiolated biotin to immobilize TRITC−extravidin proteins and RGD to immobilize HUVEC cells.[51]

Herein, we report the post-functionalization of multi-stimuli-responsive hydrogels for DIW 3D printing. Poly(isopropyl-*stat*-ethyl glycidyl ether)-*block*-poly(ethylene oxide)-*block*-poly(isopropyl-*stat*-ethyl glycidyl ether) (polymer **1**; 1.6k-8k-1.6k for the respective blocks) was synthesized and modified with methacrylate end groups to create polymer **2**. These polymer **2** based hydrogels demonstrated temperature-dependent equilibrium swelling ratios (ESRs) consistent with lower critical solution temperature (LCST) behavior in aqueous solution. Pyridyl disulfide urethane methacrylate (PDS-UM) monomers were successfully incorporated into polymer **2** hydrogels network and used as a platform for post-functionalization with thiol-containing molecules (Figure 1). Glutathione (GSH) was used as a small molecule probe to measure the conjugation kinetics of polymer **2**/PDS-UM hydrogels at different temperatures (5, 25, 37 °C) and swelling states (as-cured/preswollen). Other thiol-containing molecules (small molecules, polymer, and protein) were also conjugated onto polymer **2** hydrogels. To demonstrate the potential for these materials, polymer **2**/PDS-UM hydrogels were DIW 3D printed, and post-

print functionalized with fluorescein thiol (FITC-SH). The differential swelling in response to environmental temperatures was also confirmed for these printed objects.

2. EXPERIMENTAL SECTION

2.1. Materials and Instrumentation. All chemicals and solvents were purchased from Sigma-Aldrich, Fisher Scientific, or Oakwood Chemical and used without further purification unless noted otherwise. CYCLO(ARG-GLY-ASP-D-PHE-CYS) (RGD-SH) was purchased from AstraTech. RGD-PEG-SH was purchased from Biochempeg Scientific. Isopropyl glycidyl ether (iPGE, 98%) and ethyl glycidyl ether (EGE, 98%) were dried over CaH2 for 24 h, distilled into a flask containing butyl magnesium chloride (2 M in tetrahydrofuran, THF), re-distilled, and stored under N_2 atmosphere. Poly(ethylene oxide) (PEO, Mn 8000 g mol-1) was dried under vacuum overnight prior to use. Dry THF was obtained using neutral alumina using a Pure Process Technology solvent purification system. A potassium naphthalenide solution (1M) was prepared by dissolving naphthalene (3.2 g) in THF (25 mL), adding potassium (0.975 g), and storing under N_2 atmosphere. All NMR spectra were obtained on a Bruker Advance 300 or 500 MHz spectrometer. All absorbance spectra were collected on either a Varian Cary 5000 UV-Vis-NIR or Agilent 8453 UV-Vis spectrophotometer.

2.2. Synthesis of HEPDS. Hydroxyethyl pyridyl disulfide was synthesized (Scheme S1) according to literature procedures. Briefly, dipyridyl disulfide (5 g, 23 mmol) and glacial acetic acid (0.6 mL) were dissolved in MeOH (60 mL). A solution of 2-mercaptoethanol (1.41 mL, 20 mmol) in MeOH (25 mL) was added dropwise to the reaction solution at over 30 min and the solution was allowed to stir at RT for 24 h. The solvent was then removed under reduced pressure and the product was redissolved in minimal ethyl acetate. The

solution was washed with deionized water (3x), dried with anhydrous sodium sulfate, and filtered. After concentrating again under reduced pressure, the product was purified via silica gel column chromatography using an ethyl acetate/hexane mixture (17:3) as the elution solvent. The product was obtained as a light-yellow oil (1.58 g, 38% yield). ^{1}H NMR (499 MHz, $CDCl_3$): δ = 8.52-8.50 (d, 1H), 7.60-7.57 (t, 1H), 7.42-7.40 (d, 1H), 7.17-7.14 (t, 1H), 3.82-3.80 (t, 2H), 2.97-2.95 (t, 2H).

2.3. Synthesis of PDS-UM. Pyridyl disulfide-urethane methacrylate (PDS-UM) was synthesized (Scheme S2) using modified literature procedures[52]. HEPDS (1.58 g, 8.44 mmol) was dissolved in dry THF (5 mL) and added to a flame dried reaction flask. 2-isocyanoethyl methacrylate (1.43 mL, 10.12 mmol) and dibutyltin dilaurate (19.75 μL) were subsequently added under inert N_2 atmosphere and the reaction mixture was allowed to stir at RT for 20 h. The solvent was then removed under reduced pressure. The impure product was redissolved in DCM and was washed with deionized water and brine. The product was purified via silica gel column chromatography using an ethyl acetate/hexane mixture (2:3) as the elution solvent. The product was obtained as a white powder (2.41 g, 88% yield). ^{1}H NMR (499 MHz, $CDCl_3$): δ = 8.48-8.47 (d, 1H), 7.70-7.62 (m, 2H), 7.11-7.08 (t, 1H), 6.12 (s, 1H), 5.60 (s, 1H), 4.99 (s, 1H), 4.34-4.32 (t, 2H), 4.24-4.21 (t, 2H), 3.51-3.47 (q, 2H), 3.05-3.03 (t, 2h), 1.95 (s, 3H). ^{13}C NMR (500 MHz, $CDCl_3$): δ = 167.3, 159.76, 156.01, 149.73, 137.06, 135.94, 126.14, 120.86, 119.86, 77.33, 77.08, 76.83, 63.64, 62.79, 40.21, 37.85, 18.33.

2.4. Preparation of Polymer 2/PDS-UM Hydrogel Solution. For the formulation of a 5 g batch of hydrogel, polymer **2** was first dissolved in deionized water at a concentration of 20 wt % polymer. The resulting polymer solution was cooled overnight at 5 °C to facilitate complete

dissolution of the polymer via LCST behavior. Using the temperature-responsive sol-gel transition of the polymer, a 0.088 M solution of PDS-UM in MeOH (100 μL) and the photo-radical initiator 2-hydroxy-2-methylpropiophenone (5 μL) were added to the sol state at 5 °C and homogenized using a vortex mixer for 30 s. The hydrogel was centrifuged (4400 rpm, 10 min) to remove bubbles.

2.5. Hydrogel Sample Preparation. Hydrogel solutions were poured into nine disk molds (r = 5 mm, h = 5 mm) and cured under 365 nm UV light for 15 min. The nine cured disks were washed with water to remove any unreacted polymer from the sample surface.

2.6. Polymer 2 Swelling Studies. The swelling rates of polymer **2** hydrogels were studied at three different temperatures (5, 25, and 37 °C) and two different swelling states (as-cured and preswollen). Three hydrogel samples were placed in scintillation vials containing deionized water at their respective temperatures and weighed at time points from 0 – 48 h. The swelling ratio was determined using the Equation (1) (Supporting Information)

2.7. 2-Pyridothione Calibration. A calibration curve was established by dissolving various concentrations of 2-pyridothione (0.01 – 0.5 mM) in deionized water and measuring the corresponding absorbance values at $\lambda = 343$ nm. A linear regression analysis of the absorbance vs concentration plot produced a linear fit with an R^2 value of 0.999.

2.8. 2-Pyridothione Release Studies. The release of 2-pyrdiothione from polymer **2**/PDS-UM hydrogels was studied at three different temperatures (5, 25, and 37 °C) and two different swelling states (as-cured and preswollen). GSH was chosen as the free-thiol reactant molecule at concentrations typically found in tumor cells (10 mM). Three hydrogel samples were placed in scintillation vials containing a GSH solution (7 mL, 10 mM in deionized water) at their respective temperatures. Periodically over the course of 96 h, aliquots were taken for UV-Vis analysis. The

percent release was determined using the absorbance at λ = 343 nm corresponding to the released 2-pyridothione and Equation (2) (Supporting Information).

2.9. Direct-write 3D Printing of Polymer 2/PDS-UM Hydrogels. A modified pneumatic direct-write 3D printer was assembled based on a Tronxy P802E 3D Printer kit, from Shenzen Tronxy Technology Co. The CAD model was designed on Fusion 360 and the G-code file was produced with Slic3r software. The hydrogel ink was cooled to 5 °C and poured into a Nordson Optimum 10 cc fluid dispensing barrel equipped with a Metcal conical (410 μm inner diameter) precision tip nozzle. The loaded syringe was warmed to ambient temperature and pressurized using nitrogen gas (20 psi) to extrude the gel from the nozzle at 5.0 mm s^{-1}. The printer was controlled with an Arduino using the Marlin firmware.

3. RESULTS AND DISCUSSION

We chose to synthesize poly(isopropyl-*stat*-ethyl glycidyl ether)-*block*-poly(ethylene oxide)-*block*-poly(isopropyl-*stat*-ethyl glycidyl ether) triblock copolymers (polymer **1**) with a 1:1 ratio of isopropyl glycidyl ether and ethyl glycidyl ether, respectively, based on the studies of our previous report on these poly(alkylene ether) triblock copolymers.[30,32] Polymer **1** was synthesized via anionic ring-opening polymerization of ethyl and isopropyl glycidyl ether initiated from poly(ethylene glycol) using potassium naphthalenide as the base (Figure 1, Supporting Information S2-S3). The chain ends were then functionalized using methacrylic anhydride to afford polymer **2**. This polymer composition affords shear-thinning hydrogels with a reversible sol-gel transition at 15.61 °C. The lower critical solution temperature (LCST) driven sol-gel transition is ideal for material processing, while the shear-thinning response enables effective extrusion-based additive manufacturing. Photo-chemical crosslinking of the material through UV-light initiated polymerization of methacrylate chain ends creates robust hydrogels capable of post-print

bioreactor applications. However, the permanent fixation of the network removes the sol-gel transition and shear-thinning response of the material, as the polymer chains are now covalently bound and no longer have the freedom to disassemble at lower temperatures or under high shear environments. Interestingly, chemically crosslinked polymers such as F127[53–55] or poly(N-isopropyl acrylamide) (PNIPAm)[56–58] are known to exhibit volume phase transitions as a result of LCST behavior. Therefore, we hypothesized that polymer **2** hydrogels would retain their temperature-responsive behavior after crosslinking, which would be reflected in the temperature dependent equilibrium swelling ratios (ESR) (Figure 2).

To investigate ESR of the cross-linked hydrogels, the samples (20 wt% polymer **2** in deionized water) were placed in aqueous solutions at 5, 25, and 37 °C and their swelling ratios were recorded periodically over 48 h (Figure 2a). At low temperatures (5 °C), the hydrogels experience enhanced swelling, achieving an ESR of 53.0 ± 0.8%. Meanwhile, at room (25 °C) or elevated (37 °C) temperatures, the material reaches an ESR of 28.5 ± 1.3 and 8.6 ± 0.8%, respectively. This was consistent with the LCST behavior of the polymer: as the temperature of the environment decreased, the system absorbed a higher volume of water as the polymer became more hydrophilic and the glycidyl ether blocks fully solvated. On the other hand, an increase in temperature caused the polymer chains to collapse as they became more hydrophobic and reduced the swelling ratio of the hydrogel. All hydrogel samples reached final ESR values after 24 h of incubation.

The ESR of the crosslinked hydrogel is reversible and showed no loss in mass or change in ESR over 5 cycles of alternating between 5 and 37 °C (Figure 2b). Hydrogel samples originally equilibrated at 5 °C experienced a drop in ESR when placed in high (37 °C) temperature environments. Once placed back into low temperature solutions, the hydrogel samples recovered back to their highly swollen state.

PDS-UM monomers were synthesized using a modified procedure[52] and copolymerized with polymer **2** to afford hydrogels that can be post-functionalized with thiol-containing molecules (Scheme S1-S2). PDS monomers are inherently hydrophobic with limited water solubility. Thus, the incorporation of this monomer into polymers and polymer networks typically require organic solvents[51,59,60] or functionalization onto hydrophilic polymers[61,62] in order to prepare PDS containing hydrogels. One unique aspect of amphiphilic triblock copolymers, such as polymer **2**, is their ability to self-assemble into flower-like micelles and encapsulate hydrophobic molecules such as PDS-UM.[63–67] The inherent sol-gel temperature transition of polymer **2** hydrogels was used to efficiently dissolve and homogenize the PDS-UM monomer at a molar ratio of 1:10 (PDS-UM:polymer **2**). The polymer **2**/PDS-UM formulation was optimized by visually comparing different concentrations of PDS-UM to ensure maximum loading within the micelles while maintaining good solubility.

Rheological characterization of polymer **2**/PDS-UM hydrogels confirmed that the incorporation of PDS-UM did not negatively impact the temperature-, shear-, or light-responsive properties of the material (Figure S1). The temperature-dependent viscoelastic character of the material was confirmed by the presence of a sol-gel transition (T = 14.32 °C) as defined by the crossover between the storage modulus (G') and the loss modulus (G") (Figure S1a). The material exhibited shear-thinning behavior as characterized by a negative correlation between viscosity and shear rate, which represents the shear-induced flow required for extrusion-based printing methods (Figure S1b). A dynamic oscillatory strain experiment demonstrated the rapid and reversible response of the material to periods of high (100%) and low (1%) strain (Figure S1c). At low strain, such as those experienced by the hydrogel before and after printing, the material exists as a gel with G' values greater than G". Under periods of high strain, such as those experienced during

extrusion, G" values were greater than G' indicating the material was able to flow. Finally, the photochemical crosslinking of the hydrogel network was confirmed by increasing G' values upon exposure to 365 nm UV light (Figure S1d). This indicates a rapid polymerization of methacrylate chain ends, the formation of chemical crosslinks, and the stiffening of the hydrogel network.

Given the temperature-responsive behavior of polymer **2**/PDS-UM hydrogels, we further investigated the effect of the thermally responsive swelling behavior upon the reactivity of the PDS-UM toward thiols. We hypothesized that the LCST response of the polymer **2** network will afford fully solvated polymer chains at lower temperatures and the exposed PDS-UM monomer would be more reactive. To test this hypothesis, as-cured polymer **2**/PDS-UM hydrogel samples were placed in pre-equilibrated solutions of glutathione (GSH) at 5, 25, and 37 °C. The conjugation of GSH with the PDS-UM monomer can be tracked by monitoring the absorbance peak of released 2-pyridothione at 343 nm. A calibration curve was established by dissolving 2-pyridothione in aqueous solutions at various concentrations (0.1-5 mM, Figure S2-S3).

An aliquot of each solution was taken at various time points over the course of 96 h and investigated by UV-Vis spectroscopy. The percent release was calculated relative to the theoretical concentration of 2-pyridothione, assuming complete reaction of all PDS-UM active sites and plotted versus time (Figure 3a). Contrary to our hypothesis, more 2-pyridothione was released from polymer **2**/PDS-UM hydrogels at low ESRs/higher temperatures than at high ESRs/lower temperatures, specifically during the early process of incubation (Table 1). For instance, the percent release of 2-pyridothione at 8 h for samples equilibrated at 37 °C was 10.8 % higher than at 25 °C and 25.2 % higher than at 5 °C. The largest difference in percent release was observed throughout the first 8 h, with statistical analysis indicating significant differences between

temperatures at almost all time points from 0.5 – 8 h (Table S1). Hydrogel samples at all temperatures approached quantitative release within the full 96 h incubation window.

These results suggest that as-cured polymer **2**/PDS-UM hydrogels do, in fact, exhibit a temperature-dependent release of 2-pyridothione, albeit with an inverse correlation between ESR and percent released. Interestingly, when hydrogel samples are preswollen before placement in reactive GSH solutions (Figure 3b), the magnitude of 2-pyridothione release is significantly diminished. Not only were percent release values lower during the early stages of release (8 h = 28.4 vs 39.5, 34.9 vs 53.9 and 34.5 vs 64.7 for 5, 25, and 37 °C, respectively) but the final maximum release values never broke 73 %. Additionally, the temperature dependent release of 2-pyridothione observed for as-cured samples is *not* observed for preswollen samples. In fact, at no time point is there a significant difference between the percent of 2-pyridothione released at 5, 25, or 37 °C (Table S2). These results suggest that the active swelling of the hydrogel network has a major impact on the magnitude and temperature dependent release of 2-pyridothione from polymer **2**/PDS-UM hydrogels.

To demonstrate the versatility of our polymer **2**/PDS-UM platform, a number of different thiol-containing molecules were conjugated to the hydrogels. The percent release of 2-pyridothione after 24 and 96 h for each compound was recorded in Table 2. Cysteamine hydrochloride and 2-mercaptoethanol (2-MCE) were chosen as model compounds to demonstrate the ability of our platform to conjugate molecules in the presence of polar hydrogen bonding functionalities (-NH_2 and -OH). RGD- SH and RGD-PEG-SH (M_n = 5,000) were included due to their cell adhesive capabilities as well as to demonstrate the ability to conjugate large polymeric compounds. Similarly, BSA (M_n = 66kD) with a single free cysteine reacted with up to 12.9% of the available PDS-UM sites. The larger macromolecules, BSA and PEG conjugated significantly less (12.9 %

and 30.9 %, respectively) than the smaller molecular probes GSH/RGD (97.9 % and 80.4 %, respectively). This can be attributed to the large increase in molecular weight (1-2 orders of magnitude) for the same number of available thiols (1) per molecule. Meanwhile, 2,2-(Ethylenedioxy)diethanethiol (EDT) and pentaerythritol tetra(3-mercaptopropionate) (PET) were incorporated to demonstrate the conjugation of multi-functional small molecules. A stoichiometric amount of EDT (2x thiol) and PET (4x thiol) relative to thiol equivalent (0.5 and 0.25 molar equivalents) were added to the reaction solution. Conjugation values of 77.4 and 33.2 % suggest that one molecule of EDT/PET is reacting multiple times, as a 1:1 conjugation ratio would yield values of 50 and 25%, respectively.

Lastly, we investigated the effect of pH upon the reaction of thiols with polymer **2**/PDS-UM. Bagiyan and co-workers previously reported that thiols can undergo spontaneous auto-oxidation in the presence of molecular oxygen in aqueous solutions. According to their results, the rate of auto-oxidation to disulfides is affected by both pH and temperature. For instance, the auto-oxidation rate of cysteamine was reportedly 15 - 20 times larger at a pH of 8.5 - 9.0 than 4 – 5, and 6 times larger at 45 °C compared to 15 °C. It was therefore necessary to modulate both the pH and temperature of our reaction solutions to suppress auto-oxidation of both the conjugating molecule as well as the 2-pyridothione leaving group. GSH, a naturally acidic compound containing two carboxylic acid moieties, undergoes efficient conjugation at pH 3 and 37 °C. Cysteamine hydrochloride, EDT, PET, RGD, and RGD-PEG-SH were reacted in solutions with the pH 5, while BSA and 2-MCE were conjugated in a phosphate buffer solution (1x PBS, pH 7.4). These compounds were therefore incubated at 25 and 5 °C, respectively, to account for the increasing basicity of the reaction solutions. All molecules were able to achieve efficient conjugation under these reaction conditions.

As a final demonstration, we 3D printed hydrogel objects that were post-print functionalized with a fluorescent dye. A customized DIW 3D printer was used to extrude hydrogel ink in a patternwise manner to create the robot figurine shown in Figure 4. The sol-gel temperature response allowed for homogenization of the PDS-UM monomer, as well as facile loading of the material into the printer syringe. The shear-thinning response facilitated the formation of rod-like filaments and enabled effective printing of the material into the computer-generated object. The post-print photochemical crosslinking allowed for handling and swelling of the object without deformation or dissolution. A thiolated fluoresceine dye (FITC-SH) was synthesized according to literature procedures[68] and conjugated to the material via thiol-reactive PDS-UM groups. The figure demonstrated high fluorescence intensity with no observable decline after successive equilibrations with fresh buffer solution. And finally, the temperature dependent ESRs allow the printed object to grow/shrink based on environmental conditions. The printed figure achieved an upper limit size of 5.2 x 7.1 cm at 5 °C (Figure 4a), and a minimum size of 4.75 x 6.34 cm at 37 °C (Figure 4b).

4. CONCLUSION

In conclusion, we developed multi-stimuli-responsive hydrogels that can be 3D printed via a direct-ink write process to afford cross-linked hydrogel networks that can be post-modified via pyridyl disulfide functionalities. Crosslinked polymer **2** hydrogel samples demonstrated temperature dependent equilibrium swelling ratios consistent with LCST behavior i.e., higher degrees of swelling at lower temperatures. PDS-UM monomers were incorporated into the network, providing the hydrogel with a thiol-reactive handle for post-functionalization. The reactivity of polymer **2**/PDS-UM hydrogels was investigated at different temperatures (5, 25, 37

°C) and swelling statuses (as-cured/preswollen). The percent release of 2-pyridothione was found to increase with temperature and in as-cured samples. The versatility of the platform was demonstrated by conjugating a diverse set of thiol-containing probes to the hydrogel including peptides, proteins, polymers, and multi-functional small molecules at various temperatures, pH values, and concentrations. Lastly, the multi-stimuli-responsive properties of the polymer **2**/PDS-UM system were demonstrated by post-functionalizing a 3D printed robot figurine. The sol-gel temperature response, shear-thinning behavior, and photochemical crosslinking properties enabled efficient DIW printing. The printed figurine was post-functionalized with the thiolated fluorescent tag, FITC-SH, and displayed changes in size induced by the temperature dependent swelling of the polymer **2** hydrogel.

AUTHOR INFORMATION

Corresponding Author

*Alshakim Nelson - Department of Chemistry, University of Washington, Seattle, WA, USA

E-mail: alshakim@uw.edu

Author Contributions

The manuscript was written through contributions of all authors. All authors have given approval to the final version of the manuscript.

Notes

The authors declare no competing financial interests.

SUPPORTING INFORMATION

Synthesis of polymer **1**/polymer **2**, synthetic scheme of HEPDS/PDS-UM, equations 1 & 2, rheological characterization of polymer **2** hydrogels and experimental details, absorbance profiles and calibration curve of 2-pyridothione in deionized water, statistical analysis for temperature dependent release of 2-pyridothione from as-cured and preswollen hydrogels, H^1 and C^{13} NMRs.

ACKNOWLEDGEMENTS

We thank Nathan Ballinger for NMR assistance and S. Cem Millik for guidance on DIW 3D printing. We gratefully acknowledge support from the National Science Foundation (1752972) for this work.

REFERENCES

(1) Spicer, C. D. Hydrogel Scaffolds for Tissue Engineering: The Importance of Polymer Choice. *Polym. Chem.* **2020**, *11* (2), 184–219.

(2) Hunt, J. A.; Chen, R.; Van Veen, T.; Bryan, N. Hydrogels for Tissue Engineering and Regenerative Medicine. *J. Mater. Chem. B* **2014**, *2* (33), 5319–5338.

(3) El-Sherbiny, I. M.; Yacoub, M. H. Hydrogel Scaffolds for Tissue Engineering: Progress and Challenges. *Glob. Cardiol. Sci. Pract.* **2013**, *2013* (3), 38.

(4) Tavakoli, S.; Klar, A. S. Advanced Hydrogels as Wound Dressings. *Biomolecules* **2020**, *10* (8), 1–20.

(5) Pan, Z.; Ye, H.; Wu, D. Recent Advances on Polymeric Hydrogels as Wound Dressings. *APL Bioeng.* **2021**, *5* (1), 11504.

(6) Jeong, B.; Kim, S. W.; Bae, Y. H. Thermosensitive Sol-Gel Reversible Hydrogels. *Adv. Drug Deliv. Rev.* **2002**, *54* (1), 37–51.

(7) Li, L.; Scheiger, J. M.; Levkin, P. A. Design and Applications of Photoresponsive Hydrogels. *Adv. Mater.* **2019**, *31* (26), 1807333.

(8) Xiao, L.; Zhu, J.; Londono, J. D.; Pochan, D. J.; Jia, X. Mechano-Responsive Hydrogels Crosslinked by Block Copolymer Micelles. *Soft Matter* **2012**, *8* (40), 10233–10237.

(9) Taki, M.; Yamashita, T.; Yatabe, K.; Vogel, V. Mechano-Chromic Protein-Polymer Hybrid Hydrogel to Visualize Mechanical Strain. *Soft Matter* **2019**, *15* (46), 9388–9393.

(10) Wang, S.; Lee, J. M.; Yeong, W. Y. Smart Hydrogels for 3D Bioprinting. *Int. J. Bioprinting* **2015**, *1* (1), 3–14.

(11) Shafranek, R. T.; Millik, S. C.; Smith, P. T.; Lee, C. U.; Boydston, A. J.; Nelson, A. Stimuli-Responsive Materials in Additive Manufacturing. *Progress in Polymer Science*. Elsevier Ltd June 1, 2019, pp 36–67.

(12) Highley, C. B.; Rodell, C. B.; Burdick, J. A. Direct 3D Printing of Shear-Thinning Hydrogels into Self-Healing Hydrogels. *Adv. Mater.* **2015**, *27* (34), 5075–5079.

(13) Ouyang, L.; Highley, C. B.; Rodell, C. B.; Sun, W.; Burdick, J. A. 3D Printing of Shear-Thinning Hyaluronic Acid Hydrogels with Secondary Cross-Linking. *ACS Biomater. Sci. Eng.* **2016**, *2* (10), 1743–1751.

(14) Mccracken, J. M.; Badea, A.; Kandel, M. E.; Gladman, A. S.; Wetzel, D. J.; Popescu, G.; Lewis, J. A.; Nuzzo, R. G. Programming Mechanical and Physicochemical Properties of 3D Hydrogel Cellular Microcultures via Direct Ink Writing. *Adv. Healthc. Mater.* **2016**, *5* (9), 1025–1039.

(15) Robert Barry III, B. A.; Shepherd, R. F.; Hanson, J. N.; Nuzzo, R. G.; Wiltzius, P.; Lewis, J. A.; Lewis, J. A.; Shepherd, R. F.; Barry III, R. A.; Wiltzius, P.; Hanson, J. N.; Nuzzo, R. G. Direct-Write Assembly of 3D Hydrogel Scaffolds for Guided Cell Growth. *Adv. Mater* **2009**, *21*, 2407–2410.

(16) Naficy, S.; Gately, R.; Gorkin, R.; Xin, H.; Spinks, G. M. 4D Printing of Reversible Shape Morphing Hydrogel Structures. *Macromol. Mater. Eng.* **2017**, *302* (1), 1600212.

(17) Bakarich, S. E.; Gorkin, R.; Panhuis, M. In Het; Spinks, G. M. 4D Printing with Mechanically Robust, Thermally Actuating Hydrogels. *Macromol. Rapid Commun.* **2015**, *36* (12), 1211–1217.

(18) Odent, J.; Vanderstappen, S.; Toncheva, A.; Pichon, E.; Wallin, T. J.; Wang, K.; Shepherd, R. F.; Dubois, P.; Raquez, J. M. Hierarchical Chemomechanical Encoding of Multi-Responsive Hydrogel Actuators: Via 3D Printing. *J. Mater. Chem. A* **2019**, *7* (25), 15395–15403.

(19) Sanchez-Rexach, E.; Smith, P. T.; Gomez-Lopez, A.; Fernandez, M.; Cortajarena, A. L.; Sardon, H.; Nelson, A. 3D-Printed Bioplastics with Shape-Memory Behavior Based on Native Bovine Serum Albumin. *ACS Appl. Mater. Interfaces* **2021**, *13* (16), 19193–19199.

(20) Wang, Y.; Miao, Y.; Zhang, J.; Wu, J. P.; Kirk, T. B.; Xu, J.; Ma, D.; Xue, W. Three-Dimensional Printing of Shape Memory Hydrogels with Internal Structure for Drug Delivery. *Mater. Sci. Eng. C* **2018**, *84*, 44–51.

(21) Shiblee, M. N. I.; Ahmed, K.; Kawakami, M.; Furukawa, H. 4D Printing of Shape-Memory Hydrogels for Soft-Robotic Functions. *Adv. Mater. Technol.* **2019**, *4* (8), 1900071.

(22) Li, H.; Go, G.; Ko, S. Y.; Park, J. O.; Park, S. Magnetic Actuated PH-Responsive Hydrogel-Based Soft Micro-Robot for Targeted Drug Delivery. *Smart Mater. Struct.* **2016**, *25* (2), 027001.

(23) Cicuéndez, M.; Doadrio, J. C.; Hernández, A.; Portolés, M. T.; Izquierdo-Barba, I.; Vallet-Regí, M. Multifunctional PH Sensitive 3D Scaffolds for Treatment and Prevention of Bone Infection. *Acta Biomater.* **2018**, *65*, 450–461.

(24) Zhang, M.; Vora, A.; Han, W.; Wojtecki, R. J.; Maune, H.; Le, A. B. A.; Thompson, L. E.; McClelland, G. M.; Ribet, F.; Engler, A. C.; Nelson, A. Dual-Responsive Hydrogels for Direct-Write 3D Printing. *Macromolecules* **2015**, *48*, 6482–6488.

(25) Kolesky, D. B.; Truby, R. L.; Gladman, A. S.; Busbee, T. A.; Homan, K. A.; Lewis, J. A. 3D Bioprinting of Vascularized, Heterogeneous Cell-Laden Tissue Constructs. *Adv. Mater.* **2014**, *26*, 3124–3130.

(26) Wong, J.; Gong, A. T.; Defnet, P. A.; Meabe, L.; Beauchamp, B.; Sweet, R. M.; Sardon, H.; Cobb, C. L.; Nelson, A. 3D Printing Ionogel Auxetic Frameworks for Stretchable Sensors. *Adv. Mater. Technol.* **2019**, *4* (9), 1900452.

(27) Wong, J.; Basu, A.; Wende, M.; Boechler, N.; Nelson, A. Mechano-Activated Objects with Multidirectional Shape Morphing Programmed via 3D Printing. *ACS Appl. Polym. Mater.* **2020**, *2* (7), 2504–2508.

(28) Basu, A.; Saha, A.; Goodman, C.; Shafranek, R. T.; Nelson, A. Catalytically Initiated Gel-in-Gel Printing of Composite Hydrogels. *ACS Appl. Mater. Interfaces* **2017**, *9* (46), 40898–40904.

(29) Karis, D. G.; Ono, R. J.; Zhang, M.; Vora, A.; Storti, D.; Ganter, M. A.; Nelson, A. Cross-Linkable Multi-Stimuli Responsive Hydrogel Inks for Direct-Write 3D Printing. *Polym. Chem.* **2017**, *8* (29), 4199–4206.

(30) Fellin, C. R.; Adelmund, S. M.; Karis, D. G.; Shafranek, R. T.; Ono, R. J.; Martin, C. G.; Johnston, T. G.; DeForest, C. A.; Nelson, A. Tunable Temperature- and Shear-Responsive Hydrogels Based on Poly(Alkyl Glycidyl Ether)S. *Polym. Int.* **2019**, *68* (7), 1238–1246.

(31) Priks, H.; Butelmann, T.; Illarionov, A.; Johnston, T. G.; Fellin, C.; Tamm, T.; Nelson, A.; Kumar, R.; Lahtvee, P. J. Physical Confinement Impacts Cellular Phenotypes within Living Materials. *ACS Appl. Bio Mater.* **2020**, *3* (7), 4273–4281.

(32) Johnston, T. G.; Fellin, C. R.; Carignano, A.; Nelson, A. Poly(Alkyl Glycidyl Ether)

Hydrogels for Harnessing the Bioactivity of Engineered Microbes. *Faraday Discuss.* **2019**, *219*, 58–72.

(33) Smith, M. L.; Heitfeld, K.; Slone, C.; Vaia, R. A. Autonomic Hydrogels through Postfunctionalization of Gelatin. *Chem. Mater.* **2012**, *24* (15), 3074–3080.

(34) Yigit, S.; Sanyal, R.; Sanyal, A. Fabrication and Functionalization of Hydrogels through "Click" Chemistry. *Chemistry - An Asian Journal*. John Wiley & Sons, Ltd October 4, 2011, pp 2648–2659.

(35) Kosif, I.; Park, E. J.; Sanyal, R.; Sanyal, A. Fabrication of Maleimide Containing Thiol Reactive Hydrogels via Diels-Alder/Retro-Diels-Alder Strategy. *Macromolecules* **2010**, *43* (9), 4140–4148.

(36) Wang, L.; Zhu, L.; Hickner, M.; Bai, B. Molecular Engineering Mechanically Programmable Hydrogels with Orthogonal Functionalization. *Chem. Mater* **2017**, *29*, 28.

(37) Iha, R. K.; Wooley, K. L.; Nyström, A. M.; Burked, D. J.; Kade, M. J.; Hawker, C. J. Applications of Orthogonal "Click" Chemistries in the Synthesis of Functional Soft Materials. *Chem. Rev.* **2009**, *109* (11), 5620–5686.

(38) Campos, L. M.; Killops, K. L.; Sakai, R.; Paulusse, J. M. J.; Damiron, D.; Drockenmuller, E.; Messmore, B. W.; Hawker, C. J. Development of Thermal and Photochemical Strategies for Thiol-Ene Click Polymer Functionalization. *Macromolecules* **2008**, *41* (19), 7063–7070.

(39) Deforest, C. A.; Polizzotti, B. D.; Anseth, K. S. Sequential Click Reactions for Synthesizing and Patterning Three-Dimensional Cell Microenvironments. *Nat. Mater.* **2009**, *8* (8), 659–664.

(40) Altin, H.; Kosif, I.; Sanyal, R. Fabrication of "Clickable" Hydrogels via Dendron-Polymer Conjugates. *Macromolecules* **2010**, *43* (8), 3801–3808.

(41) Altinbasak, I.; Arslan, M.; Sanyal, R.; Sanyal, A. Pyridyl Disulfide-Based Thiol-Disulfide Exchange Reaction: Shaping the Design of Redox-Responsive Polymeric Materials. *Polymer Chemistry*. Royal Society of Chemistry December 28, 2020, pp 7603–7624.

(42) Zugates, G. T.; Anderson, D. G.; Little, S. R.; Lawhorn, I. E. B.; Langer, R. Synthesis of Poly(β-Amino Ester)s with Thiol-Reactive Side Chains for DNA Delivery. *J. Am. Chem. Soc.* **2006**, *128* (39), 12726–12734.

(43) Duvall, C. L.; Convertine, A. J.; Benoit, D. S. W.; Hoffman, A. S.; Stayton, P. S. Intracellular Delivery of a Proapoptotic Peptide via Conjugation to a RAFT Synthesized Endosomolytic Polymer. *Mol. Pharm.* **2010**, *7* (2), 468–476.

(44) Ju, Y.; Zhang, M.; Zhao, H. Poly(ϵ-Caprolactone) with Pendant Natural Peptides: An Old Polymeric Biomaterial with New Properties. *Polym. Chem.* **2017**, *8* (35), 5415–5426.

(45) Keller, S.; T.wilson, J.; Patilea, G. I.; Kern, H. B.; Convertine, A. J.; Stayton, P. S. Neutral

Polymer Micelle Carriers with PH-Responsive, Endosome-Releasing Activity Modulate Antigen Trafficking to Enhance CD8+ T Cell Responses. *J. Control. Release* **2014**, *191*, 24–33.

(46) Bontempo, D.; Heredia, K. L.; Fish, B. A.; Maynard, H. D. Cysteine-Reactive Polymers Synthesized by Atom Transfer Radical Polymerization for Conjugation to Proteins. *J. Am. Chem. Soc.* **2004**, *126* (47), 15372–15373.

(47) Matsumoto, N. M.; González-Toro, D. C.; Chacko, R. T.; Maynard, H. D.; Thayumanavan, S. Synthesis of Nanogel-Protein Conjugates. *Polym. Chem.* **2013**, *4* (8), 2464–2469.

(48) Heredia, K. L.; Nguyen, T. H.; Chang, C. W.; Bulmus, V.; Davis, T. P.; Maynard, H. D. Reversible SiRNA-Polymer Conjugates by RAFT Polymerization. *Chem. Commun.* **2008**, No. 28, 3245–3247.

(49) Vázquez-Dorbatt, V.; Tolstyka, Z. P.; Chang, C. W.; Maynard, H. D. Synthesis of a Pyridyl Disulfide End-Functionalized Glycopolymer for Conjugation to Biomolecules and Patterning on Gold Surfaces. *Biomacromolecules* **2009**, *10* (8), 2207–2212.

(50) Gunasekaran, K.; Nguyen, T. H.; Maynard, H. D.; Davis, T. P.; Bulmus, V. Conjugation of SiRNA with Comb-Type PEG Enhances Serum Stability and Gene Silencing Efficiency. *Macromol. Rapid Commun.* **2011**, *32* (8), 654–659.

(51) Gevrek, T. N.; Cosar, M.; Aydin, D.; Kaga, E.; Arslan, M.; Sanyal, R.; Sanyal, A. Facile Fabrication of a Modular "Catch and Release" Hydrogel Interface: Harnessing Thiol-Disulfide Exchange for Reversible Protein Capture and Cell Attachment. *ACS Appl. Mater. Interfaces* **2018**, *10* (17), 14399–14409.

(52) Li, L.; Liu, X.; Xu, J.; Kan, C. Microfluidic Preparation of Thiol-Containing Monodisperse Polymer Microspheres and Their Adsorption of Pb2+ in Water. *Chem. Eng. J.* **2019**, *375*, 122012.

(53) Song, L.; Zhang, B.; Gao, G.; Xiao, C.; Li, G. Single Component Pluronic F127-Lipoic Acid Hydrogels with Self-Healing and Multi-Responsive Properties. *Eur. Polym. J.* **2019**, *115*, 346–355.

(54) Zhao, S.; Cao, M.; Wu, J.; Xu, W. Synthesis and Characterization of Biodegradable Thermo- Ad PH-Sensitive Hydrogels Based on Pluronic F127/Poly(ε-Caprolactone) Macromer and Acrylic Acid. *Macromol. Res.* **2009**, *17* (12), 1025–1031.

(55) Zhu, W.; Wang, B.; Zhang, Y.; Ding, J. Preparation of a Thermosensitive and Biodegradable Microgel via Polymerization of Macromonomers Based on Diacrylated Pluronic/Oligoester Copolymers. *Eur. Polym. J.* **2005**, *41* (9), 2161–2170.

(56) Wu, T. Y.; Zrimsek, A. B.; Bykov, S. V.; Jakubek, R. S.; Asher, S. A. Hydrophobic Collapse Initiates the Poly(N -Isopropylacrylamide) Volume Phase Transition Reaction Coordinate. *J. Phys. Chem. B* **2018**, *122* (11), 3008–3014.

(57) Okudan, A.; Altay, A. Investigation of the Effects of Different Hydrophilic and Hydrophobic Comonomers on the Volume Phase Transition Temperatures and Thermal Properties of N-Isopropylacrylamide-Based Hydrogels. *Int. J. Polym. Sci.* **2019**, *2019*, 7324181.

(58) Xu, X.; Liu, Y.; Fu, W.; Yao, M.; Ding, Z.; Xuan, J.; Li, D.; Wang, S.; Xia, Y.; Cao, M. Poly(N-Isopropylacrylamide)-Based Thermoresponsive Composite Hydrogels for Biomedical Applications. *Polymers*. MDPI AG March 1, 2020, p 580.

(59) Chien, H. W.; Xu, X.; Ella-Menye, J. R.; Tsai, W. B.; Jiang, S. High Viability of Cells Encapsulated in Degradable Poly(Carboxybetaine) Hydrogels. *Langmuir* **2012**, *28* (51), 17778–17784.

(60) Perera, M. M.; Ayres, N. Gelatin Based Dynamic Hydrogels: Via Thiol-Norbornene Reactions. *Polym. Chem.* **2017**, *8* (44), 6741–6749.

(61) Choh, S. Y.; Cross, D.; Wang, C. Facile Synthesis and Characterization of Disulfide-Cross-Linked Hyaluronic Acid Hydrogels for Protein Delivery and Cell Encapsulation. *Biomacromolecules* **2011**, *12* (4), 1126–1136.

(62) Zhang, Y.; Heher, P.; Hilborn, J.; Redl, H.; Ossipov, D. A. Hyaluronic Acid-Fibrin Interpenetrating Double Network Hydrogel Prepared in Situ by Orthogonal Disulfide Cross-Linking Reaction for Biomedical Applications. *Acta Biomater.* **2016**, *38*, 23–32.

(63) Cabral, H.; Miyata, K.; Osada, K.; Kataoka, K. Block Copolymer Micelles in Nanomedicine Applications. *Chemical Reviews*. American Chemical Society July 25, 2018, pp 6844–6892.

(64) Xu, W.; Ling, P.; Zhang, T. Polymeric Micelles, a Promising Drug Delivery System to Enhance Bioavailability of Poorly Water-Soluble Drugs. *J. Drug Deliv.* **2013**, *2013*, 1–15.

(65) Kumi, B. C.; Hammouda, B.; Greer, S. C. Self-Assembly of the Triblock Copolymer 17R4 Poly(Propylene Oxide)-Poly(Ethylene Oxide)-Poly(Propylene Oxide) in D2O. *J. Colloid Interface Sci.* **2014**, *434*, 201–207.

(66) Nguyen-Misra, M.; Mattice, W. L. Micellization and Gelation of Symmetric Triblock Copolymers with Insoluble End Blocks. *Macromolecules* **1995**, *28*, 1444–1457.

(67) Chu, B.; Liu, T.; Wu, C.; Zhou, Z.; Mark Nace, V. Structures and Properties of Block Copolymers in Solution. *Macromol. Symp.* **1997**, *118* (1), 221–227.

(68) Park, S.; Foote, P. K.; Krist, D. T.; Rice, S. E.; Statsyuk, A. V. UbMES and UbFluor: Novel Probes for Ring-between-Ring (RBR) E3 Ubiquitin Ligase PARKIN. *J. Biol. Chem.* **2017**, *292* (40), 16539–16553.

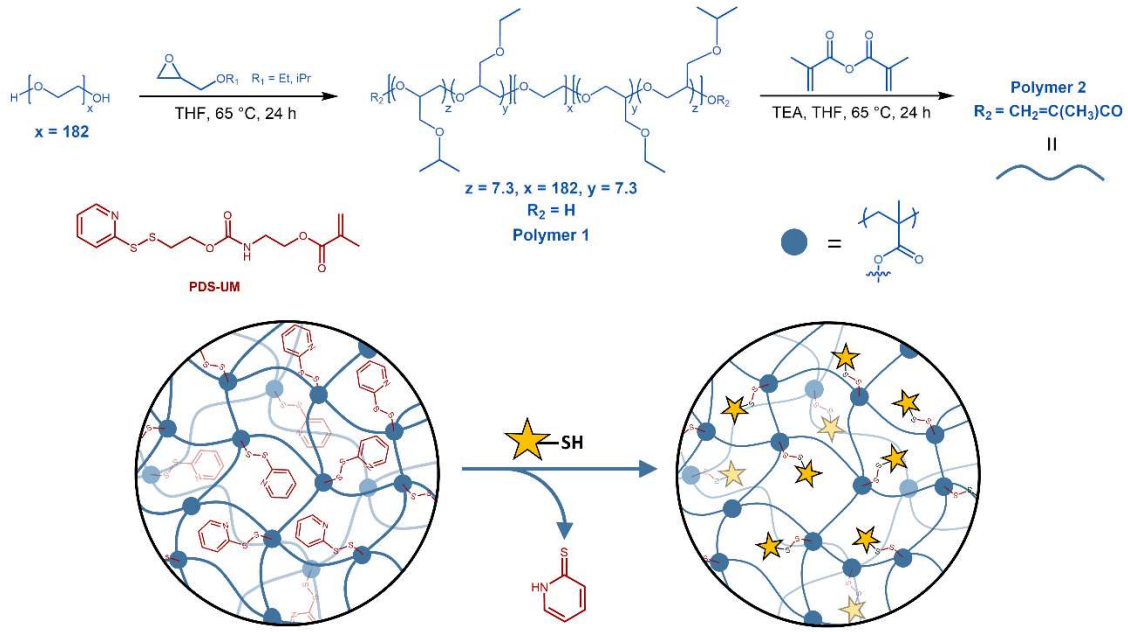

Figure 1. Synthesis of polymer **2** and graphical representation of the post-functionalization of polymer **2**/PDS-UM hydrogels with thiol-containing molecules.

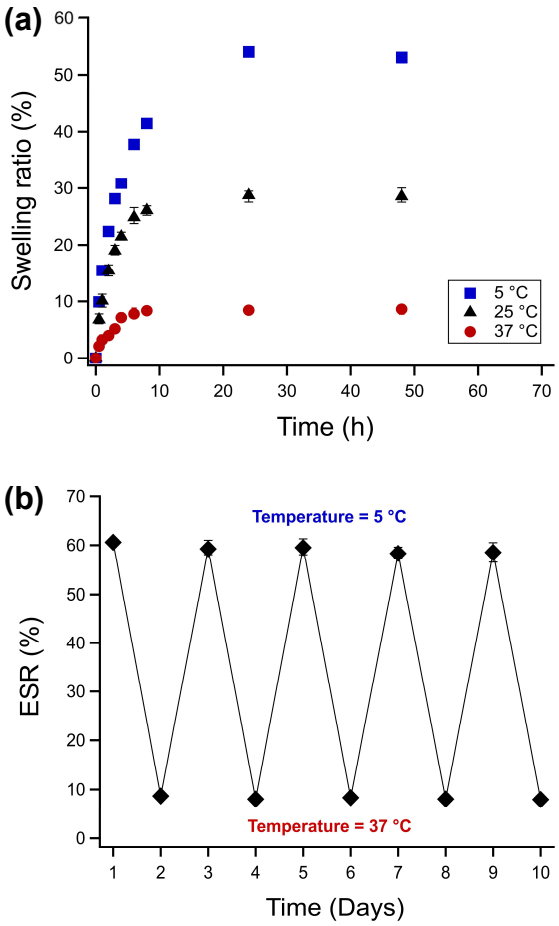

Figure 2. (a) Swelling ratio (%) vs Time (h) for polymer **2**/PDS-UM samples at 5 (blue squares), 25 (black triangles), and 37 °C (red circles). (b) Demonstration of reversible swelling from 5 °C to 37 °C over ten days.

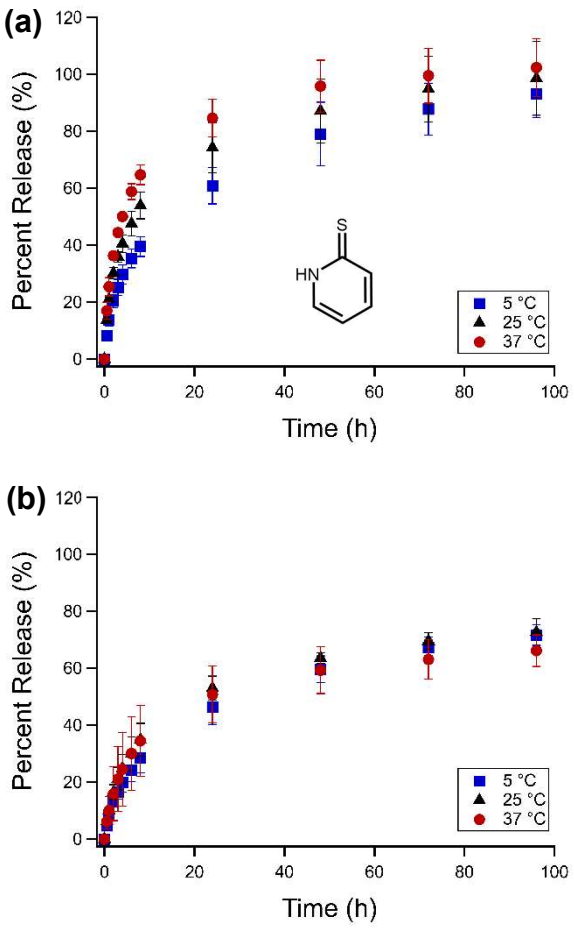

Figure 3. Percent release of 2-pyridothione (%) vs time (h) for (a) as-cured and (b) preswollen polymer **2**/PDS-UM samples at 5 (blue squares), 25 (black triangles), and 37 °C (red circles).

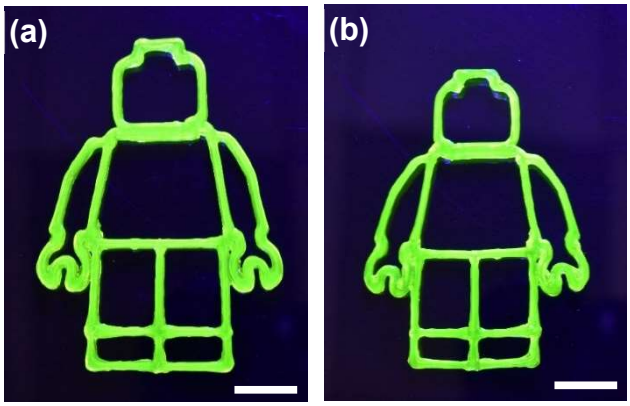

Figure 4. A 3D printed robot figurine was printed using a pneumatic DIW 3D printer with a 0.41 mm inner diameter nozzle and printing speed 5.0 mm/s. The FITC-SH was conjugated to the printed polymer network to demonstrate the functionalization as evidenced by the observed fluorescence. The figurine was also swollen at (a) 5 °C and (b) 37 °C to demonstrate the temperature dependent swelling of the polymer **2**/PDS-UM system (scale bar = 1 cm).

Table 1. Percent release of 2-pyridothione from crosslinked polymer **2**/PDS-UM hydrogels at different temperatures (5, 25, or 37 °C), swelling status (as cured versus preswollen), and time points (24/96 h).

Temperature (°C)	Swelling status	8 h (%)[a,b]	96 h (%)[a,b]
5	Preswollen	28.4 ± 5.2	71.6 ± 3.6
5	As-cured	39.5 ± 3.5	93.1 ± 8.2
25	Preswollen	34.9 ± 5.8	72.6 ± 4.7
25	As-cured	53.9 ± 4.7	98.5 ± 13.0
37	Preswollen	34.5 ± 12.4	66.1 ± 5.5
37	As-cured	64.7 ± 3.5	102.3 ± 10.2

[a] Calculated using Equation (2) (Supporting Information)

[b] Error given as standard deviation over 3 replicate experiments

Table 2. Conjugation of thiol-containing molecules to polymer **2**/PDS-UM hydrogels. The percent release of 2-pyridothione was determined via UV-Vis spectroscopy at 24 and 96 h.

Molecule	% Release (24 h)[a]	% Release (96 h)[a]	Equivalents	pH	Temperature (°C)
GSH	79.3	97.9	40	3	37
Cysteamine	80.9	77.0	40	5	25
EDT	80.4	77.5	0.5	5	25
PET	30.3	33.2	0.25	5	25
RGD-SH	71.6	80.4	5	5	25
RGD-PEG-SH	24.3	30.9	5	5	25
2-MCE	87.5	90.2	40	7.4	5
BSA	10.1	12.9	1	7.4	5

[a] Calculated using Equation (2) (Supporting Information)